International Journal of Control, Automation, and Systems (2015) 13(3):680-688 ISSN:1598-6446 eISSN:2005-4092
DOI 10.1007/s12555-013-0092-y http://www.springer.com/12555

A Simplified Approach to Assessment of Mission Success for Helicopter Landing on a Ship

Jongki Moon*, Jean Charles Domercant, and Dimitri Mavris

Abstract: In this paper, operation of a helicopter near a ship is statistically investigated to provide an estimate of the probability of successfully recovering manned rotorcraft on the deck of a moving ship. To this end, pitch, roll, and heave motion of the ship are calculated according to sea states. In addition, effect on dynamics of the rotorcraft from ship airwake is also considered in a simplified way. By assuming that a helicopter can land on a ship if a pilot maintains relative position and attitude difference within the safe boundary for a given time, the operational limits are probabilistically determined in terms of pilot's workload for a specified mission. The simulation environment consists of linearized helicopter dynamics, an optimal pilot model, effect of turbulent ship airwake, and ship motion. Control activities of the piloted helicopter for position holding with respect to the moving ship are transformed to generalized workload ratings. Simulation results show the proposed approach can evaluate and predict mission success rates for various operational combinations, allowing implementation into the overall effectiveness assessment of the ship and ship-helicopter combination.

Keywords: Dynamic interface, helicopter landing, pilot control model, ship motion, workload rating.

ACRONYMS

WOD	Wind over the Deck
CFD	Computational Fluid Dynamics
ADS	Aeronautical Design Standard
HQR	Handling Quality Rating
MTE	Mission Task Element
SHOL	Ship/Helicopter Operating Limit
PSD	Power Spectral Density
JONSWAP	Joint North Sea Wave Project
RMS	Root Mean Square
RPM	Revolutions Per Minute
OCM	Optimal Control Model
LQ	Linear Quadratic
WR	Workload Rating
CG	Center of Gravity

1. INTRODUCTION

From a systems point of view, the effectiveness of naval assets can be greatly increased by the inclusion of air assets. In mission effectiveness studies, the effectiveness of a naval ship can often times be doubled (e.g., search and rescue, anti-submarine warfare, maritime interdiction operations) if a rotorcraft can be deployed and recovered from the ship. However, ship-based rotorcraft operations continue to be of significant concern to both military and civilian operators.

While rotorcraft play a significant role in at-sea operations, the launch and recovery of rotorcraft under at-sea conditions can prove challenging. Turbulence in the ship-induced airwake causes a time-dependent disturbance rejection task for the pilot. Meanwhile, the interaction of the rotor and rotor wake with the ship's turbulent airwake can cause undesired and uncomfortable aircraft motion and also dangerously high pilot workload. If the workload is unacceptably high as the pilot attempts to control the vehicle, the helicopter pilot is not able to achieve a safe landing on the deck of the ship.

In addition to the complex aerodynamic environment, the motions of the ship also increase the level of difficulty in conducting onboard operations with aerial vehicles. Thus, over the past few decades there has been a significant amount of research devoted to clearly understanding helicopter and ship motions as well as the aerodynamic interactions between the two. These aerodynamic interactions, in particular, result in a dynamic coupling between the helicopter and ship, and is usually referred to as the dynamic interface. References [1,2] show detailed analyses of the complex aerodynamic coupling between the helicopter, the ship, and the atmosphere.

Successfully predicting the safe operation of ship-based rotorcraft requires determining the maximum limitations of the helicopter in the presence of a ship. This limit is usually called the WOD envelope. A larger

Manuscript received March 3, 2013; revised January 27, 2014 and May 29, 2014; accepted August 22, 2014. Recommended by Editor Hyouk Ryeol Choi.

This research was supported by the United States Office of Naval Research under Contract N00014-11-1-0443. The authors wish to thank Dr. Ronald A. Hess of UC Davis and Dr. Alan Brown of Virginia Tech for providing valuable comments and feedback regarding the modeling of ship motions.

Jongki Moon, Jean Charles Domercant, and Dimitri Mavris are with the School of Aerospace Engineering, Georgia Institute of Technology, Atlanta, Georgia 30332, USA (e-mails: {jongki.moon, jean.domercant, dimitri.mavris}@asdl.gatech.edu).
* Corresponding author.

envelope allows greater operational capability. However, obtaining this envelope is not an easy task and can prove costly and time consuming. This is due to a number of reasons. First, sufficiently modeling the dynamic interface can require extensive computational power, especially since high-fidelity CFD models must be created. Secondly, it can easily be expected that a tremendous number of evaluation tests have to be performed for various ship-helicopter combinations in order to establish the WOD envelope for all possible conditions. Moreover, if human pilots are involved this increases the complexity of the analysis; Since one is attempting to decide the very edge of the envelope, there may be safety issues associated with such experiments. Therefore, it is necessary to have the capability to predict in advance the performance of a given heliopter/ship combination.

Due to the aformentioned reasons, there currently exists a well-established methodology for evaluating the stability and control characteristics of rotorcraft, yet estimating the likelihood that ship-based rotorcraft operations can be carried out safely is seldom assessed. US Army ADS-33 sets forth the standards for rotorcraft handling qualities as well as measures for flying qualities [3]. Within [3], there are also evaluation procedures of HQRs for a set of standard maneuvers termed MTEs. HQRs are typically rated on a scale of 1-10 by human subject pilots, but also require piloted simulation facilities with expensive hardware in order to conduct the analysis [4]. Furthermore, there is a well developed body of research focused on the development of robust controllers so that a pilot's workload can be reduced and the operational boundaries are expanded [5].

The quantified evaluation of flying characteristics mentioned above are usually only focused on the rotorcraft perspective, not the combined system perspective. This means that analysts recognize that the effectiveness of naval assets can be greatly increased by the addition of rotorcraft, but no analysis is conducted to estimate the likelihood that such benefits will be realizable. Thus, it is necessary to provide a quantitative estimate for the successful operation of ship-based rotorcraft by considering environmental conditions, both ship and helicopter dynamics, and the pilot's responses. With this in mind, it is attractive to consider the feasibility of providing a preliminary evaluation methodology using desktop simulation based on simplified mathematical modeling. The problem that arises, however, is how to accomplish this early in the design process when there is the least amount of knowledge regarding rotorcraft/ship interactions. These interactions undoubtedly will impact rotorcraft handling qualities and pilot workload.

In this study, a simplified approach to the assessment of mission success for helicopter landings on a ship is developed, making it possible to determine upfront the maximum boundaries for current vehicles as well as new acquisitions. This represents various combinations of helicopter and ship operations. As reviewed in [4], however, previous studies on the helicopter/ship operations usually aim to support flight tests or build flight simulators by using higher fidelity models of specific combinations of these components. This paper considers parameterized ship characteristics, sea states, operating conditions, and pilot skill levels. In addition, two helicopters with different handling characteristics are also included for comparison. The objective of the study is to develop a probabilistic evaluation environment that supports decision-making at the early stage of the design process. Thus, the operational perspectives associated with the effectiveness of a helicopter/ship combination can be taken into account throughout the system design. The primary benefit is that the WOD envelope can be defined well within the margins of safety in terms of pilot workload. Similarly, SHOLs can be determined and used to define operational safety requirements for a given pilot, vehicle, and ship during various operating conditions [6].

This paper is organized as follows: Section 2 explains all modeling components included in the simulation environment, Section 3 provides a discussion about the criteria used in determining mission success, simulation results are shown in Section 4, and conclusions are given in Section 5.

2. MODELING COMPONENTS OF THE DYNAMIC INTERFACE

A simulation environment for helicopter landings on a ship includes the wave-induced ship motions, the helicopter dynamics, aerodynamic coupling, a human pilot representation, and sea states. In this section, each component will be explained in detail.

2.1. Ship motion

Reference [7] shows closed-form expressions describing ship motions caused by various sea states. These formulas depend only on the key dimensions of the ship: length, breadth, block coefficient, and forward speed. On the other hand, a more detailed calculation of the ship motions induced by the sea wave can be performed by taking into account the hull form, the mass distribution, and the operational profile [8,9]. However, this may prove too time-consuming and not very useful in the conceptual design phase. Therefore, in this study, the simplified method in [7] is directly taken so as to provide a rational and efficient prediction of the wave-induced motion with sufficient engineering accuracy in the early stage of the design phase.

The ship motions considered in this paper include heave, pitch, and roll motion of a monohull ship characterized by ship size, geometry, speed, and heading. PSD of each motion can be obtained by

$$\Phi_m(\omega) = \left|H_m(j\omega)\right|^2 S(\omega), \tag{1}$$

where $\Phi_m(\omega)$ represents the PSD of each motion, $H_m(\omega)$ is the frequency response function of the motion, and $S(\omega)$ the PSD of the sea wave. Since the frequency response functions rely on values of the ship characte-

Table 1. Modeling variables for ship characteristics.

	Definition
T	Mean draft (m)
B_0	Maximum waterline breadth (m)
C_b	Block coefficient
L	Length at waterline (m)
β	Heading angle with respect to the wave
V	Ship velocity (m/s)
T_N	Roll time constant (s)
GM_T	Transverse metacentric height (m)
μ	Percentage critical damping

ristics, the resulting PSDs of the ship motions reflect the design variables of the ship. Furthermore, it is noted that one cannot generate time histories of the ship motion by means of spectral factorization [10]. Thus, based on the assumption that the vertical (heave and pitch) and roll motions can be decoupled, PSDs of heave, pitch, and roll are obtained separately. Table 1 lists definitions of variables associated with the ship characteristics.

In particular, inputs for the frequency response functions of heave and pitch motions are self-explanatory, and the results show fairly good correlation with outputs of the frequency response functions and experimental data [7]. In the meantime, an approximation for roll motion requires more variables such as the roll mode time constant, the transverse metacentric height, and an empirical correction to match actual responses. The percentage critical damping μ is used to artificially increase the roll damping in the calculations [7].

It now becomes necessary to convert the PSDs of the heave, pitch, and roll motion to the time histories so as to simulate the ship motion over time. Reference [10] shows a technique for generating the time histories by using the sum of a finite number of sinusoidal signals.

To this end, the first thing to do is to integrate the PSD over frequency. Then, one can select frequencies ω_1 and ω_n as follows:

$$\int_0^{\omega_1} \Phi_m(s)\,ds = 0.05 \int_0^{\infty} \Phi_m(s)\,ds, \tag{2}$$

$$\int_0^{\omega_n} \Phi_m(s)\,ds = 0.99 \int_0^{\infty} \Phi_m(s)\,ds. \tag{3}$$

Now, $\omega_2, \cdots, \omega_{n-1}$ can be equally distributed between ω_1 and ω_n. Amplitudes a_k at the select frequencies are obtained as follows:

$$a_k = \left(2 \int_{\omega_{k-1}}^{\omega_k} \Phi_m(s)\,ds\right)^{1/2}, \quad k = 1, 2, \cdots, n. \tag{4}$$

Equations (2)~(4) imply that the PSDs calculated in (1) are represented as the sum of n sinusoidal signals, whose amplitudes are condensed so that the frequency distribution over power closely match that of the integrated PSD. However, it should be noted that information on the relative phase of each motion's time history is lost with this technique. In the end, though, one can obtain heave (h_s), pitch (θ_s), and roll (ϕ_s) of the ship in the form of time series. In this paper, motion variables of a ship follow the definitions and sign conventions given in [12].

2.2. Sea waves

The stochastic properties of ocean waves can be modeled by the generalized JONSWAP wave spectrum depending on the wave frequency ω, the significant wave height H_s, the zero-upcrossing period T_z, and the peak enhancement factor γ. In this study, the standard JONSWAP model is used by setting γ equal to 3.3. Detailed information about the wave spectrum model can be found in [7]. In addition, based on relative frequency of occurrence given in [11], ranges of H_s and T_z are chosen to be 1 to 7 meters and 5 to 10 seconds, respectively.

2.3. Helicopter model

The helicopter models used in this paper include the BO-105 and PUMA. It is assumed that the helicopter starts at a trim condition near a landing pad so that a linearized dynamic model can be used for the simulation. Using a linear interpolation, trim data for each helicopter can be obtained from [13], and the state-space representation can be expressed by

$$\dot{X}(t) = AX(t) + BU(t), \tag{5}$$

where

$$X(t) = [u \quad w \quad q \quad \theta \quad v \quad p \quad r \quad \phi \quad \psi]^T, \tag{6}$$

$$U(t) = [\delta_c \quad \delta_{lon} \quad \delta_{lat} \quad \delta_p]^T. \tag{7}$$

It can be noted from (6) that rotor flapping angles are not included in the state vector based on the quasi-steady approximation [14]. This means that a coupling between rotor and fuselage is neglected for a simplified approach to the integrated simulation. In (7), δ_c, δ_{lon}, δ_{lat}, and δ_p depict the collective input, the longitudinal cyclic input, the lateral cyclic input, and the pedal input, respectively. In this paper, a non-zero trim speed is selected according to the results from Refs. [2,15], which will be explained later. A second-order transfer function is also used for the control actuator dynamics as follows:

$$G_{act}(s) = \frac{30^2}{s^2 + 2(0.75)30s + 30^2}. \tag{8}$$

2.4. Turbulence model

A helicopter is required to operate in the atmospheric turbulence caused by the disturbed air stream around box-like structures on the deck. Besides this, the strong air stream generated by the rotor wake also changes the air flow over the deck. Thus, there exists a mutual aerodynamic coupling between a helicopter and a ship. However, high-fidelity analysis tools to support complete understanding of the coupled aerodynamics may take excessive time and cost at the early stage of the system design. Therefore, a simplified approach will be taken by making use of results from Refs. [2,15]. Experimental

results show that there exists an approximate ratio among mean wind speed (V), mean wind speed at the landing pad (V_r), and the RMS turbulence (σ_t) as follows:

$$V : V_r : \sigma_t = 1 : 0.4 \sim 0.58 : 0.05 \sim 0.13. \tag{9}$$

In (9), the values of V_r and the RMS value of gust speed are about 50% and 10% of the speed of the ship, respectively. This also explains why a nonzero trim speed is chosen for a linearized helicopter dynamic model. In addition, it is assumed that there are no steady crosswinds over the deck.

Furthermore, the effect of turbulent airwake on the helicopter dynamics can be represented by the undesired and unexpected imposition of rotor control inputs. NASA Ames Research Center performed flight tests for the UH-60 and provided deterministic transfer functions representing relationships between turbulence and control inputs [15]. For example, equation (10) represents the deflection angle of the main rotor collective input due to the turbulent air as follows:

$$\left.\frac{\delta_c}{w_t}(s)\right|_{\text{UH-60}} = 0.149\sigma_t^{-0.7069}\sqrt{\frac{3\sigma_t^2 V_r}{\pi \ R_m}} \left[\frac{s+33.91\dfrac{V_r}{R_m}}{\left(s+1.46\dfrac{V_r}{R_m}\right)\left(s+9.45\dfrac{V_r}{R_m}\right)}\right], \tag{10}$$

where R_m is the main rotor radius and w_t is a white noise signal with unity covariance. In addition, it is possible to obtain approximate expresstions for different helicopters by the scaling procedures found in [16]. Assuming that the same ratio of V, V_r, and σ_t is applicable to different helicopters, controller deflections due to the turbulence are scalable using the main rotor radius (R_m) and the rotor RPM (Ω). For example, the effect on the main rotor collective control of BO-105 can be given by

$$\left.\frac{\delta_c}{w_t}(s)\right|_{\text{BO-105}} = \left.\frac{\delta_c}{w_t}(s)\right|_{\text{UH-60}} \cdot H(s, R_m, V_r), \tag{11}$$

$$H(s, R_m, V_r) = \frac{\left.\dfrac{(\pi V_r / 8R_m)}{s+(\pi V_r / 8R_m)} R_m\Omega\right|_{\text{BO-105}}}{\left.\dfrac{(\pi V_r / 8R_m)}{s+(\pi V_r / 8R_m)} R_m\Omega\right|_{\text{UH-60}}}. \tag{12}$$

Similarly, expressions for different control inputs of different helicopters are obtained.

2.5. Pilot model

During recovery procedures, the pilot is required to maintain a relative position with respect to the moving landing spot as desired. It is possible that pilots can wait for a quiescent period in ship motion while hovering at a prescribed height over the deck. Reference [17] presents a way to predict the motion of a landing pad so as to catch the quiescent moment, but the relative position change due to the aerodynamic coupling is not considered for the motion prediction. In this paper, it is assumed that the pilot is tasked with tracking the changing position of the landing pad. Since pilot behavior is time-varying, adaptive, and nonlinear by nature, there exist several ways to model human manual-control activities [4]. Among those, the OCM of a human pilot is chosen in this paper because of its computational efficiency and wide applicability. A pilot is modeled using the LQ Gaussian formulation so as to regulate the disturbing effect of turbulence over the deck [1].

In this paper, to represent the OCM of the human pilot, the LQ tracking problem is considered in conjunction with the linearized helicopter model given in (5)~(7). This formulation is based on two clear reasons: First, the turbulence effect is separately included in the simulation environment in the form of an undesired control deflection. Secondly, the pilot is asked to follow the landing spot position. The reference command will be the position of the landing pad observed by the pilot, and the objective will be to find a compensator that minimizes the quadratic performance index given by

$$J = \int_0^\infty \left\{(CX - r_c)^T Q(CX - r_c) + U^T RU\right\} dt, \tag{13}$$

where r_c represents the position change of the landing spot. A solution for the LQ tracking problem can be expressed by [20]

$$U = -KX + R^{-1}B^T\lambda, \tag{14}$$

$$K = R^{-1}B^T S, \tag{15}$$

$$0 = A^T S + SA - SBR^{-1}B^T S + C^T QC, \tag{16}$$

$$0 = (A - BK)^T \lambda + C^T Qr_c. \tag{17}$$

As shown in (14), the control inputs have a feedforward term as well as a feedback term. In addition, control inputs are passed through a model of the neuromotor dynamics [1], which represents the physiological limitations on the ability of human pilots, given by

$$G_{nm}(s) = \frac{1}{\tau_{nm}s + 1}. \tag{18}$$

In (18), a time constant τ_{nm} is usually identified as 0.2 [21]. In this paper, it is assumed that τ_{nm} can adequately depict the skill level of the pilot. During the simulation, mean value of τ_{nm} is given a range from 0.2 to 0.6.

3. DECISION CRITERIA FOR MISSION SUCCESS

Once every component is modeled within the integrated environment, one can obtain ship motion variables, helicopter motion variables, and control inputs applied by the pilot for a given combination. Fig. 1 represents the integrated environment for assessing mission effectiveness. In order to determine whether the results are acceptable for the recovery mission, the first thing to consider is the task performance and pilot workload.

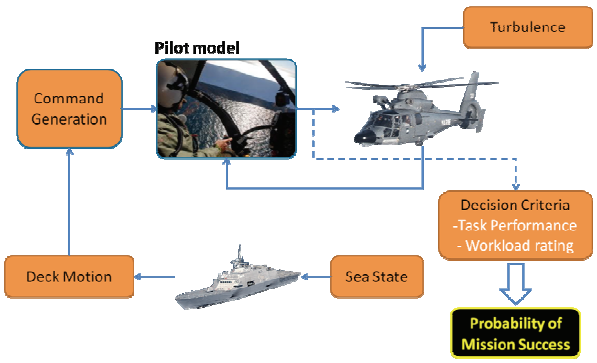

Fig. 1. Dynamic interface simulation environment.

3.1. Task performance

The effectiveness of pilot's control activities can be measured by tracking errors. This implies that the task is considered a mission failure when the tracking error goes beyond the boundary value. To this end, a rectangular parallelepiped can be imposed as a maximum tolerance. The size of the imaginary rectangular parallelepiped may vary according to the location of the landing spot, the helicopter size, and the deck size. Relative attitude as well as relative position is important in deciding mission success, because a larger difference in attitude may result in a higher possibility of inclined landing. The main task of the pilot is assumed to be to track the deck position, and attitude angles of the ship are not of primary interest. However, since a helicopter needs to tilt its attitude to generate desired accelerations, attitude difference may be significant despite small position errors. In addition, lack of visibility during the mission can be included in the assessment by reducing the size of the rectangular parallelepiped.

3.2. Pilot workload

Besides a system of vehicles, the pilot's perspective is also important for the evaluation of the limits early in the design cycle for shipboard operations of rotorcraft. It is possible that the pilot's efforts are totally different for similar maximum tracking errors. This means that the emphasis may be solely on workload if the performance level is the same. In addition, there exists physical limitations on enduring fatigue due to an excessive workload. Therefore, the maximum pilot workload becomes an important criterion for determining mission success.

Reference [22] developed a methodology associated with the workload questionnaire, and [23] suggested a predictor of the workload in the form of a polynomial regression model. However, the regression model in [23] shows negative sensitivities to some control activities, which contradicts a general tendency in pilot's workload. In this paper, a neural-net based model is used to predict pilot workload using four control surface positions and speeds as inputs. An increase in rapid control movements reflects a growing workload, and a larger control surface deflection requires a larger control stick force [13]. In particular, the standard deviation and the standard deviation of the rate of control inputs are correlated with the pilot workload. Since the motion of the landing spot is very close to a sinusoidal signal, averaged values of control inputs do not seem to be significant [23]. Thus, the WR can be expressed by

$$WR = \max\left\{ f_i\left(\bar{\mu}_i\right)\right\}, \quad i = 1,2,\cdots,8, \tag{19}$$

where

$$f_i\left(\bar{\mu}_i\right) = \frac{10}{1+\exp(c_i - \bar{\mu}_i)}, \tag{20}$$

$$\bar{\mu} = \left[\sigma(U)^T \quad \sigma(\dot{U})^T\right]^T. \tag{21}$$

The principal idea behind (19) is that the most difficult pilot activity out of all control channels is a dominant contributor to the WR. In addition, as shown in (20), a sigmoid function is used to determine difficulty level of each control activity. In order to consider the fact that the highly skilled pilot can endure a wider range of control stick changes, the centroid c_i decreases as the time constant of the pilot neuromotor in (18) increases. By doing this, a pilot model with a smaller time constant results in a smaller WR for same control activities.

4. SIMULATION RESULTS

4.1. Simulation setup

Once the ship motion variables heave (h_s), pitch (θ_s), and roll (ϕ_s) are obtained, vertical (h_l) and lateral (s_l) position changes of the landing spot are calculated as follows:

$$\begin{aligned} h_l = h_s &+ \sqrt{x_l^2 + z_l^2}\sin\theta_s \\ &+ \sqrt{y_l^2 + z_l^2}\left(\cos\alpha_l - \cos\left(\alpha_l + \phi_s\right)\right), \end{aligned} \tag{22}$$

$$s_l = \sqrt{y_l^2 + z_l^2}\left(\sin\left(\alpha_l + \phi_s\right) - \sin\alpha_l\right), \tag{23}$$

where $\left(x_l, y_l, z_l\right)$ denote the location of the landing spot from the CG of the ship, and $\alpha_l = \tan^{-1}(y_l / z_l)$. In order to calculate aerodynamic properties of the selected helicopter, the ratio in (9) is selected to be 1:0.5:0.1.

4.2. Test case evaluation

In order to evaluate the feasibility of the integrated simulation environment developed in this paper, an example case is taken from [7]. A TMV114 fast ferry is modeled, with the main parameters as follows: L = 96m, B_0 = 13.8m, T = 2.5m, C_b = 0.53, T_N = 6.3s, GM_T = 4.19m, β = 135°(180° corresponds to a head sea), and V=20 knots. In addition, the value for μ is selected to be 0.4 so as to match the experimental roll motion data. The location of the landing spot is assumed to be $(0.6L,\ 0,3T)$. The significant wave height H_s = 2m and the zero-upcrossing period T_z = 9 s is chosen since this condition occurs most frequently. A dynamic model of the BO-105 helicopter is linearized at 10 knots forward speed according to the assumed ratio. The pilot response delay τ_{nm} in (18) randomly changes during the simulation, with a mean of 0.2s and standard deviation of 0.1s. All

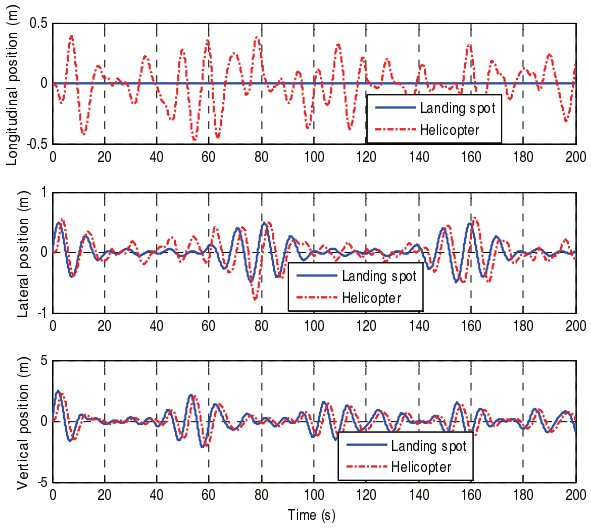

Fig. 2. Position comparison of the landing spot and the helicopter.

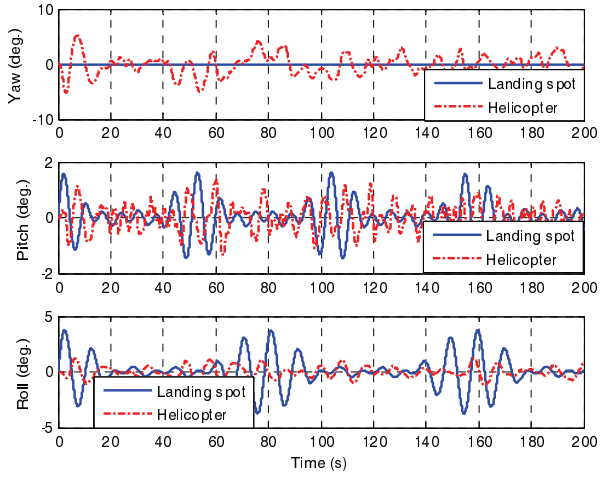

Fig. 3. Attitude comparison of the landing spot and the helicopter.

positions and attitudes for the BO-105 helicopter are set to zero initially.

Position changes of the landing spot and the helicopter are compared in Fig. 2. The longitudinal position change of the landing spot is assumed to be negligible so that it remains at zero. As shown in Fig. 2, the heave motion along the vertical axis is the largest displacement change. Fig. 3 compares attitude changes of the ship and the helicopter. Yaw angle of the ship is also assumed to stay unchanged. Yaw angle of the helicopter shows the largest changes, and pitch angle of the helicopter changes most rapidly. As explained in Section 3.1, the pilot is supposed to primarily track the landing spot. In order to achieve position tracking, the helicopter needs to tilt its attitude angles. Thus, attitude difference is imposed as auxiliary criteria of task performance. As a result, Fig. 2 shows that the helicopter tracks well the landing spot, while maintaining attitude difference small enough for the recovery task as seen in Fig. 3. Both the control inputs and their rates applied by the pilot model are

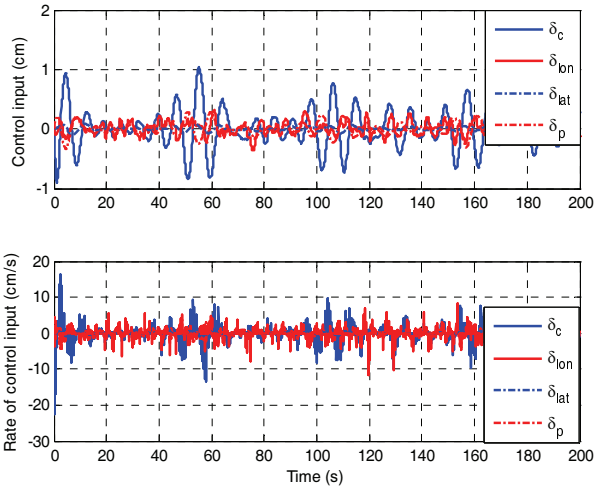

Fig. 4. Histories of control inputs and their rates.

shown in Fig. 4. As mentioned before, collective control and longitudinal cyclic control are more actively involved and a pilot needs to endure the workload associated with these control activities. According to (19), the WR turns out to be 3.88.

4.3. Model validation

Every component of the dynamic interface modeling in this study is integrated by means of simplification and parameterization for the purpose of analyzing system effectiveness. Even though all simplified components are previously validated, it is important to check if any unexpected coupling effects occur during the system integration. Therefore, it is required to prove that the simplified approach presented in this paper shows agreeable correlation with actual phenomena during the helicopter landing on the deck. In this section, the system validation is performed by comparing the results of the proposed environment with those of high fidelity simulations and/or flight experiments.

An adaptive airwake compensator is designed for dynamic interface of the combination of UH-60 and USS Saipan [24]. In [24], pilot workloads and helicopter locations resulted from piloted simulation-based evaluations are presented to show the effectiveness of the airwake compensator for a 29th order linearized helicopter model. In order to run a case in the environment developed in this study, the following ship parameters are used: $L = 250$m, $B_0 = 32$m, $T = 7.9$m, $C_b = 0.67$, $T_N = 24.9$s, GM_T=1.5m, $\beta = 0^o$, and V = 0 knots. Landing spot 8 on the deck is assumed to be located at $(0.7L, 0.4B_0, 1.5T)$. Furthermore, a linearized model of the UH-60 at hover is obtained from [25], and the value of V_r is chosen to be 10 knots.

Fig. 5 shows distributions of maximum tracking errors and the WR of 200 simulation runs with the proposed method in this paper. Mean values of maximum position errors are 1.75m, 1.58m, and 1.84m, respectively. It is also observed that the averaged WR is 3.35. In addition, a piloted test for the 10 knot head wind condition is presented in [24]. It can be seen that that maximum

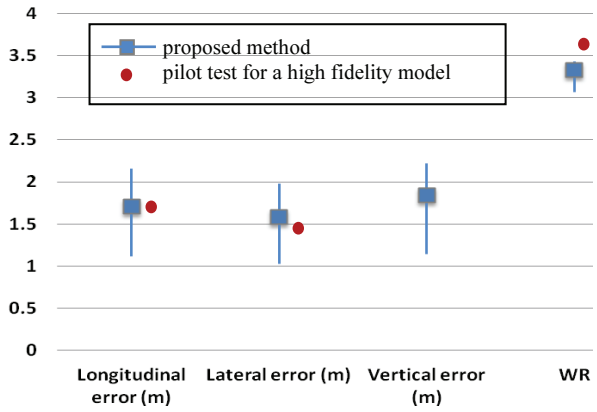

Fig. 5. Comparison of proposed method to high fidelity modeling.

position errors along the longitudinal and lateral directions from the piloted test are about 1.8m and 1.5m, respectively. The averaged WR is about 3.7. Unfortunately, vertical position errors are not presented in [24]. As shown in Fig. 5, it can be concluded that the proposed method shows fairly acceptable agreement with the piloted simulation test using the high-fidelity helicopter model.

4.4. Assessment of mission success

In this section, the decision criteria proposed in Section 3 have been applied to various combinations of ship design parameters, sea states, helicopter types, and pilot skills. In addition, the maximum limits of position and attitude difference may vary depending on different operating conditions. In this paper, the width, depth, and height of the imaginary rectangular parallelepiped for maximum tracking errors are set to $0.2B_o$, $0.03L$, and R_m, respectively [1]. Performance criteria for yaw, pitch, and roll difference are set to $\pm 10^o$, $\pm 5^o$, and $\pm 5^o$, respectively [11]. In addition, the maximum WR is assumed to be bounded to a value of 5 as expected in [26]. In general, HQR for a recovery landing is expected to be near 5 [13]. For a given operating combination, 1000 cases are simulated with randomly selected initial conditions of the helicopter within the criteria. As a result, a mission success rate can be represented by the ratio of the number of cases satisfying all criteria to the total number of cases.

Tables 2~6 show representative results for various design parameter combinations. Table 2 lists the results of the case shown in Section 4.2 and Table 3 shows the case where $\beta = 180^o$. Comparing Tables 2 and 3 shows that the helicopter has a better chance of landing safely on the deck when the ship aligns itself in the direction of the oncoming seas. The results of a PUMA-TMV114 combination is also summarized in Table 4. Table 5 shows the results of the case where a pilot of a BO-105 helicopter tries to land on a ship with different characteristic values. It can be seen that a certain combination of ship design variables shows more robust responses so that the mission success rate may improve for more expected sea states. In addition, Table 6 shows

Table 2. Mission success rate of BO-105 ($L = 96$ m, $B_0 = 13.8$ m, $T = 2.5$ m, $C_b = 0.53$, $T_N = 6.3$ s, $GM_T = 4.19$ m, $\beta = 135^o$, $\tau_{nm} = 0.2$ s).

		H_s (m)						
		1	2	3	4	5	6	7
T_z (s)	5	1.00	1.00					
	6	1.00	1.00	0.12	0.03	0.00	0.00	
	7	1.00	1.00	0.06	0.00	0.00	0.00	0.00
	8	1.00	0.88	0.08	0.00	0.00	0.00	0.00
	9	1.00	0.89	0.10	0.01	0.00	0.00	0.00
	10	1.00	1.00	0.10	0.01	0.00	0.00	0.00

Table 3. Mission success rate of BO-105 ($L = 96$ m, $B_0 = 13.8$ m, $T = 2.5$ m, $C_b = 0.53$, $T_N = 6.3$ s, $GM_T = 4.19$ m, $\beta = 180^o$, $\tau_{nm} = 0.2$ s).

		H_s (m)						
		1	2	3	4	5	6	7
T_z (s)	5	1.00	1.00					
	6	1.00	1.00	1.00	0.53	0.35	0.25	
	7	1.00	1.00	1.00	0.34	0.11	0.00	0.00
	8	1.00	1.00	0.88	0.21	0.06	0.00	0.00
	9	1.00	1.00	1.00	0.58	0.00	0.00	0.00
	10	1.00	1.00	1.00	0.93	0.13	0.00	0.00

Table 4. Mission success rate of PUMA ($L = 96$ m, $B_0 = 13.8$ m, $T = 2.5$ m, $C_b = 0.53$, $T_N = 6.3$ s, $GM_T = 4.19$ m, $\beta = 180^o$, $\tau_{nm} = 0.2$ s).

		H_s (m)						
		1	2	3	4	5	6	7
T_z (s)	5	1.00	1.00					
	6	1.00	1.00	1.00	1.00	0.84	0.30	
	7	1.00	1.00	1.00	0.87	0.41	0.05	0.02
	8	1.00	1.00	1.00	0.18	0.03	0.02	0.00
	9	1.00	1.00	1.00	0.89	0.01	0.00	0.00
	10	1.00	1.00	1.00	0.89	0.24	0.00	0.00

Table 5. Mission success rate of BO-105 ($L = 150$ m, $B_0 = 17.0$ m, $T = 5.0$ m, $C_b = 0.53$, $T_N = 15$ s, $GM_T = 2.0$ m, $\beta = 180^o$, $\tau_{nm} = 0.2$ s).

		H_s (m)						
		1	2	3	4	5	6	7
T_z (s)	5	1.00	1.00					
	6	1.00	1.00	1.00	1.00	1.00	0.91	
	7	1.00	1.00	1.00	0.91	0.67	0.59	0.52
	8	1.00	1.00	0.96	0.54	0.28	0.21	0.19
	9	1.00	1.00	1.00	0.38	0.23	0.18	0.14
	10	1.00	1.00	1.00	0.42	0.26	0.18	0.16

Table 6. Mission success rate of BO-105 ($L = 150$ m, $B_0 = 17.0$ m, $T = 5.0$ m, $C_b = 0.53$, $T_N = 15$ s, $GM_T = 2.0$ m, $\beta = 180^o$, $\tau_{nm} = 0.5$ s).

		H_s (m)						
		1	2	3	4	5	6	7
T_z (s)	5	1.00	1.00					
	6	1.00	1.00	0.93	0.69	0.55	0.48	
	7	1.00	0.93	0.61	0.51	0.44	0.35	0.29
	8	1.00	0.63	0.34	0.20	0.11	0.01	0.00
	9	1.00	0.57	0.38	0.24	0.15	0.08	0.00
	10	1.00	0.68	0.40	0.25	0.15	0.11	0.05

the results for a case where a less skilled pilot operates the helicopter. It is clearly shown that pilot skill is also important in determining the success rate. The authors realize that the results may more accurately reflect the real task when prediction and tracking of the deck motion are simultaneously implemented as a pilot model.

5. CONCLUSIONS

A simplified approach for assessing and predicting mission success rates of helicopter landings on ship decks is studied in this paper. Closed-form expressions of ship motion dependent upon ship design characteristics and sea states are implemented in the simulation. Linearized helicopter models and wind-over-the-deck statistical data are used to represent a simplified helicopter dynamics model. In addition, the effects of turbulent air flow on the helicopter are modeled as undesired control surface movements. A pilot is modeled by a LQ tracking controller in conjunction with the neuromotor dynamics. Criteria to decide mission success are set by position error, attitude difference, and workload rating. Simulation results of various combinations of ship, helicopter, and pilot demonstrate the feasibility of the proposed technique for evaluating and predicting mission success rates. In addition, this simulation environment can be used at the early stage of the ship design process, particularly when mission effectiveness is considered as one of the performance criteria.

The results of this simplified approach should be compared with those of more detailed modeling methods and components. For example, dynamic influence from the rotor flapping angles, the effect of crosswinds over the deck, and the flight mode transition from approach to station keeping need to be considered for further investigation. It is also expected that parameterized simulations would be useful for easy integration into an overall analysis tool by means of generating a surrogate model of the mission success rate.

REFERENCES

[1] D. Lee, N. Sezer-Uzol, J. Horn, and L. N. Long, "Simulation of helicopter shipboard launch and recovery with time-accurate airwake," *Journal of Aircraft*, vol. 42, no. 2, pp. 448-461, March 2005.

[2] J. V. Healy, "Establishing a database for flight in the wake of structures," *Journal of Aircraft*, vol. 29, no. 4, pp. 559-564, 1992.

[3] U. S. Army Aviation and Missile Defense Command, *Aeronautical Design Standard, Performance Specification, Handling Qualities Requirements for Military Rotorcraft*, U. S. Army Aviation and Missile Defense Command, Redstone Arsenal, AL, 2000.

[4] S. K. Advani and C. H. Wilkinson, "Dynamic interface modeling and simulation - a unique challenge," *Proc. of Royal Aeronautical Society Conference on Helicopter Flight Simulation*, November 2001.

[5] J. Cooper, J. Schierman, and J. Horn, "Robust Adaptive Disturbance Compensation for Ship-based Rotorcraft," *Proc. of the AIAA Guidance, Navigation, and Control Conference*, August 2010.

[6] G. P. Turner, R. Bradley, and G. Brindley "Simulation of pilot control activity for the prediction of workload ratings in helicopter/ship operations," *Proc. of the 26th European Rotorcraft Forum*, September 2000.

[7] J. J. Jensen, A. E. Mansour, and A. S. Olsen, "Estimation of ship motion using closed-form expressions," *Ocean Engineering*, vol. 31, no. 1, pp. 61-85, 2004.

[8] K. J. Rawson and E. C. Tupper, *Basic Ship Theory*, Butterworth-Heinemann, Boston, MA, 2001.

[9] J. N. Newman, "The theory of ship motions," *Advances in Applied Mechanics*, vol. 18, pp. 221-283, 1978.

[10] R. A. Hess, "Application of a model-based flight director design technique to a longitudinal hover task," *Journal of Aircraft*, vol. 14, no. 3, pp. 265-271, 1977.

[11] R. A. Hess, "Simplified technique for modeling piloted rotorcraft operations near ships," *Journal of Guidance, Control, and Dynamics*, vol. 29, no. 6, pp. 1339-1349, 2006.

[12] T. I. Fossen, *Guidance and Control of Ocean Vehicles*, John Wiley & Sons, Chichester, West Sussex, 1994.

[13] G. D. Padfield, *Helicopter Flight Dynamics: The Theory and Application of Flying Qualities and Simulation Modeling*, AIAA, Reston, Virginia, 1996.

[14] M. B. Tischler and M. G. Cauffman, "Frequency-response methods for rotorcraft system identification: flight applications to BO-105 coupled rotor/fuselage dynamics," *Journal of the American Helicopter Society*, vol. 37, no. 1, pp. 3-17, 1992.

[15] J. A. Lusardi, *Control Equivalent Turbulence Inputs Model for the UH-60*, Ph.D. Dissertation, Department of Mechanical and Aeronautical Engineering, University of California, Davis, 2004.

[16] R. A. Hess, "A simplified and approximate technique for scaling rotor control inputs for turbulence modeling," *Journal of the American Helicopter Society*, vol. 49, no. 3, pp. 361-366, 2004.

[17] X. Yang, "Displacement motion prediction of a landing deck for recovery landing of rotary UAVs," *International Journal of Control, Automation, and Systems*, vol. 11, no. 1, pp. 58-64, 2013.

[18] R. J. Jagacinski and J. M. Flach, *Control Theory for Humans-Quantitative Approaches to Modeling Performance*, Erlbaum, Mahwah, NJ, 2003.

[19] D. L. Kleinman, S. Baron, and W. H. Levison, "An optimal control model of human response part I: theory and validation," *Automatica*, vol. 6, no. 3, pp. 357-369, 1970.

[20] F. L. Lewis and V. L. Syrmos, *Optimal Control*, John Wiley & Sons, New York, NY, 1995.

[21] D. M. Pool, P. M. T. Zaal, M. M. van Paassen, and M. Mulder, "Identification of multimodal pilot

models using ramp target and multisine disturbance signals," *Journal of Guidance, Control, and Dynamics*, vol. 34, no. 1, pp. 86-97, 2011.
[22] C. A. Macdonald, *The Development of an Objective Methodology for the Prediction of Helicopter Pilot Workload*, Ph.D. Dissertation, Department of Mathematics, Glasgow Caledonian University, 2001.
[23] R. Bradley, C. A. Macdonald, and T. W. Buggy, "Quantification and prediction of pilot workload in the helicopter/ship dynamic interface," *Proc. of the Institution of Mechanical Engineers*, October 2005.
[24] J. Cooper, J. Schierman, J. Horn, T. Yomchinda, and E. O'Neill, "Handling qualities evaluation of an adaptive disturbance compensation system for ship-based rotorcraft," *Proc. of the 67th American Helicopter Society Forum*, May 2011.
[25] J. Fletcher, *A Model Structure for Identification of Linear Models of the UH-60 Helicopter in Hover and Forward Flight*, NASA Technical Memorandum 110362, August 1995.
[26] D. G. Mitchell, T. K. Nicoll, M. A. Fallon, and S. H. Roark, "Rotorcraft handling qualities for shipboard operations," *Proc. of AIAA Atmospheric Flight Mechanics Conference*, August 2009.

Jongki Moon received his Ph.D. degree in Aerospace Engineering from the Georgia Institute of Technology, Atlanta in 2009. He has worked as Postdoctoral fellow at Aerospace Systems Design Laboratory in Georgia Tech. He also earned the B.S. and M.S. degrees in Aerospace Engineering from Seoul National University, Korea, in 1998 and 2000, respectively. His research interests include adaptive control, intelligent system, and multi-agent control.

Jean Charles Domercant is Research Faculty at the Georgia Institute of Technology School of Aerospace Engineering, where he oversees Defense & Space related research in the Aerospace Systems Design Laboratory (ASDL). He holds a BS in Aerospace Engineering (2000) from the University of Illinois Urbana-Champaign, an ME in Engineering Management (2006) from Old Dominion University, an MS in Aerospace Engineering (2008) and a Ph.D. in Aerospace Engineering (2011) from the Georgia Institute of Technology. His research interests include missile defense, technology portfolio selection, defense acquisitions and decision making, command & control and architecture-based systems-of-systems engineering.

Dimitri Mavris is the Boeing Regents Professor of Advanced Aerospace Systems Analysis at the Guggenheim School of Aerospace Engineering, Georgia Institute of Technology, and the director of its Aerospace Systems Design Laboratory (ASDL). Under Professor Mavris' direction, ASDL performs wide-ranging technical research with a focus on the formulation, development and implementation of comprehensive approaches to the design of affordable and high quality complex systems using visual analytics and virtual experimentation. He received his B.S., M.S., and Ph.D. degrees in Aerospace Engineering from the Georgia Institute of Technology in 1984, 1985, and 1988, respectively.